

Jet Damping of a Solid Rocket: Theory and Flight Results

W. T. THOMSON*

University of California, Los Angeles, Calif.

AND

G. S. REITER†

TRW Space Technology Laboratories, Redondo Beach, Calif.

The angular motion of a spin stabilized solid rocket is computed, considering the effect of jet damping about axes normal to the spin axis. The approximate formula used is chosen for computational accuracy and to fit the rocket geometry. Results are compared with measurements of body angular acceleration made during the rocket's flight in space. The comparison indicates that the jet damping is a very strong effect in this case, and that the approximate formula gives adequate accuracy for computing the reduction in conical precession motion due to jet damping. It is probable that the same formula can be used to estimate jet damping for other solid rockets.

I. Introduction

THE term jet damping refers to the change in the angular rates of a thrusting rocket due to the torques exerted by the gases flowing out the nozzle. The jet damping effect is especially important in spin stabilized rockets where it acts to reduce the amplitude of the conical free precession motion and, therefore, to reduce the motion to a steady spin. It is important to know what the cone angle is at staging, as this strongly influences the attitude error of the next stage. In rockets operating in air, jet damping is usually second in importance to aerodynamic moments. In vacuum, however, the jet damping can be the most important torque acting on the rocket.

Several simplified theories have been proposed to give estimates of the rate of damping for a particular rocket.¹⁻⁵ In general, these theories use one-dimensional gas flow in the rocket and characterize the thrust chamber and nozzle by certain approximate dimensions. Proper verification of these approximate theories has been difficult to obtain because of the lack of experimental data on the attitude of a spinning rocket in vacuum flight.

In the present paper, a formula for pitch jet damping is derived from the general rocket equations in a body-fixed coordinate system assuming one-dimensional flow. The formula is selected to use quantities that are known accurately and to be compatible with the geometry of the rocket considered.

The formula, a modification of the one presented in Ref. 4, is evaluated to give the predicted rate of cone angle damping for a particular frequently used spin-stabilized rocket, the Allegany Ballistics Laboratory† X-248 with a satellite payload. The resulting prediction of jet damping is then compared with measurements of the angular motion made in actual flight.

II. Conclusions

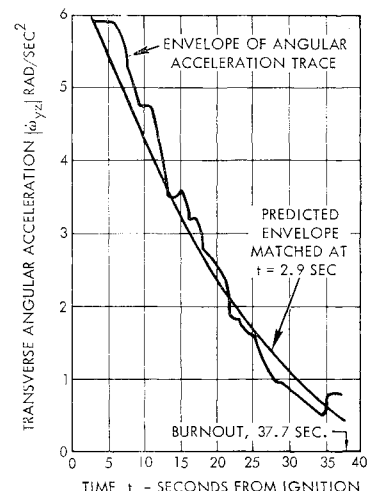
The results of the comparison of theory and experiment, shown in Fig. 1, indicate that 1) jet damping is a very strong effect for the X-248 rocket; 2) the formula chosen gives excellent agreement with the flight data, even though the

Received April 22, 1964; revision received September 14, 1964.

* Professor of Engineering; also Consultant, TRW Space Technology Laboratories.

† Assistant Manager, Dynamics Department. Member AIAA.

Fig. 1 Explorer VI third-stage flight: envelope of oscillatory portion of transverse angular acceleration illustrating jet damping.



rocket internal geometry and gas flow are represented only approximately; and 3) it is highly probable that the same formula will predict accurately the jet damping rates for other solid rockets with similar internal geometry.

III. Analytical Prediction of Motion

A. Vector Equations of Motion

We take as a system the mass m within a closed boundary around the rocket. Since mass flows across this boundary, the system is a variable mass system.

Position within the rocket is defined in terms of body coordinates xyz attached to it. The angular velocity and angular acceleration of the xyz coordinate system are ω and $\dot{\omega}$, respectively, and the position of its origin O is defined by the vector R_0 , measured from a fixed reference. (Boldface symbols denote vector and dyadic quantities.) The center of mass of the system is then designated by \bar{r} measured from the moving origin O (Fig. 2).

The mass of the rocket at any time t is m , and, since the system is losing mass, \dot{m} is negative. When a mass m_j is

‡ The authors wish to acknowledge the kindness of the Allegany Ballistics Laboratory in releasing their rocket data for public presentation.

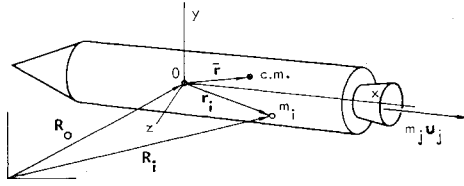


Fig. 2 Coordinate system.

ejected across the boundary, \mathbf{u}_j is its velocity vector relative to the local velocity $\dot{\mathbf{R}}_j$ of the boundary.

The reaction of the ejected masses m_j on the system is a force $\mathbf{T} = \sum m_j \mathbf{u}_j$ that can be considered together with the external applied forces \mathbf{F} and the external applied moments \mathbf{M} .

The general system is shown in Fig. 2 where m_i is one of the internal particles and m_j a particle that is being ejected. The absolute acceleration of each m_i is

$$\ddot{\mathbf{R}}_i = \ddot{\mathbf{R}}_0 + \dot{\boldsymbol{\omega}} \times \mathbf{r}_i + \boldsymbol{\omega} \times (\boldsymbol{\omega} \times \mathbf{r}_i) + [\ddot{\mathbf{r}}_i] + 2\boldsymbol{\omega} \times [\dot{\mathbf{r}}_i] \quad (1)$$

where $[\dot{\mathbf{r}}_i]$ and $[\ddot{\mathbf{r}}_i]$ are the velocity and acceleration of m_i relative to the xyz coordinate system. The force and moment equations for the whole body are then simply written as

$$\mathbf{F} = m\{\ddot{\mathbf{R}}_0 + \boldsymbol{\omega} \times (\boldsymbol{\omega} \times \bar{\mathbf{r}}) + \dot{\boldsymbol{\omega}} \times \bar{\mathbf{r}} + 2\boldsymbol{\omega} \times [\dot{\bar{\mathbf{r}}}] + [\ddot{\bar{\mathbf{r}}}]\} - \sum_j \dot{m}_j \mathbf{u}_j \quad (2)$$

$$\mathbf{M}_0 = -\ddot{\mathbf{R}}_0 \times m\bar{\mathbf{r}} + \mathcal{J} \cdot \dot{\boldsymbol{\omega}} + \boldsymbol{\omega} \times \mathcal{J} \cdot \boldsymbol{\omega} + \sum_i \mathbf{r}_i \times m_i [\ddot{\mathbf{r}}_i] + 2 \sum_i \mathbf{r}_i \times (\boldsymbol{\omega} \times m_i [\dot{\mathbf{r}}_i]) - \sum_j \mathbf{r}_j \times \dot{m}_j \mathbf{u}_j \quad (3)$$

In these equations

$$\begin{aligned} \sum_j \dot{m}_j \mathbf{u}_j &= \mathbf{T} = \text{thrust reaction of the ejected particles on the system} \\ \sum_j \mathbf{r}_j \times \dot{m}_j \mathbf{u}_j &= \mathbf{M}_T = \text{moment of the thrust on the system} \\ -\ddot{\mathbf{R}}_0 \times m\bar{\mathbf{r}} &= \text{moment due to origin 0 not coinciding with the center of mass} \\ \mathcal{J} &= \text{moment of inertia dyadic} \\ \mathbf{F} &= \text{external force} \\ \mathbf{M}_0 &= \text{external moment about 0} \end{aligned}$$

The two terms $\mathcal{J} \cdot \dot{\boldsymbol{\omega}}$ and $\boldsymbol{\omega} \times \mathcal{J} \cdot \boldsymbol{\omega}$ correspond to the Euler equations for a constant mass system, and the moments due to the relative velocity and relative acceleration

$$\sum_i \mathbf{r}_i \times m_i [\dot{\mathbf{r}}_i] + 2 \sum_i \mathbf{r}_i \times (\boldsymbol{\omega} \times m_i [\dot{\mathbf{r}}_i])$$

are responsible for the jet damping of the rocket.

If we transfer the thrust \mathbf{T} and its moment to the left side of the equation as applied force and applied moment on the system, Eqs. (2) and (3) can be rewritten as

$$\mathbf{F} + \mathbf{T} = m\{\ddot{\mathbf{R}}_0 + \boldsymbol{\omega} \times (\boldsymbol{\omega} \times \bar{\mathbf{r}}) + \dot{\boldsymbol{\omega}} \times \bar{\mathbf{r}} + 2\boldsymbol{\omega} \times [\dot{\bar{\mathbf{r}}}] + [\ddot{\bar{\mathbf{r}}}]\} \quad (4)$$

$$\mathbf{M} + \mathbf{M}_T = -\ddot{\mathbf{R}}_0 \times m\bar{\mathbf{r}} + \text{"Euler equation"} + \text{jet damping} \quad (5)$$

where

$$\begin{aligned} \text{"Euler equation"} &= \mathcal{J} \cdot \dot{\boldsymbol{\omega}} + \boldsymbol{\omega} \times \mathcal{J} \cdot \boldsymbol{\omega} \\ \text{jet damping} &= \sum_i \mathbf{r}_i \times m_i [\ddot{\mathbf{r}}_i] + 2 \sum_i \mathbf{r}_i \times (\boldsymbol{\omega} \times m_i [\dot{\mathbf{r}}_i]) \end{aligned}$$

An alternate form of the equations can be obtained by introducing the identities

$$(d/dt)(\mathcal{J} \cdot \boldsymbol{\omega}) = \mathcal{J} \cdot \dot{\boldsymbol{\omega}} + \boldsymbol{\omega} \times \mathcal{J} \cdot \boldsymbol{\omega} + [\dot{\mathcal{J}}] \cdot \boldsymbol{\omega} \quad (6)$$

$$\begin{aligned} [\dot{\mathcal{J}}] \cdot \boldsymbol{\omega} &= \sum_i [\dot{\mathbf{r}}_i] \times m_i (\boldsymbol{\omega} \times \mathbf{r}_i) + \\ &\quad \sum_i \mathbf{r}_i \times (\boldsymbol{\omega} \times m_i [\dot{\mathbf{r}}_i]) + \sum_i \mathbf{r}_i \times \dot{m}_i (\boldsymbol{\omega} \times \mathbf{r}_i) \quad (7) \end{aligned}$$

Placing all the terms of Eqs. (6) and (7) on the left side so that the right side is zero, and adding this zero into the moment equation, the appearance of the moment equation can be changed to

$$\begin{aligned} \mathbf{M} + \mathbf{M}_T &= -\ddot{\mathbf{R}}_0 \times m\bar{\mathbf{r}} + \frac{d}{dt} (\mathcal{J} \cdot \boldsymbol{\omega}) + \\ &\quad \boldsymbol{\omega} \times \sum_i \mathbf{r}_i \times m_i [\dot{\mathbf{r}}_i] + \sum_i \mathbf{r}_i \times m_i [\ddot{\mathbf{r}}_i] - \\ &\quad \sum_i \mathbf{r}_i \times \dot{m}_i (\boldsymbol{\omega} \times \mathbf{r}_i) \quad (8) \end{aligned}$$

It should be noted here that $(d/dt)(\mathcal{J} \cdot \boldsymbol{\omega})$ contains a term that involves the differentiation of the moment of inertia, whereas in the previous moment equation there are no terms containing $\dot{\mathcal{J}}$. If we assume the jet to be symmetrical about the x axis and consider $[\dot{\mathbf{r}}_i]$ to be unidimensional along the longitudinal axis of the rocket engine core, then

$$\sum_i \mathbf{r}_i \times m_i [\dot{\mathbf{r}}_i]$$

is zero, and hence the remaining term

$$-\sum_i \mathbf{r}_i \times \dot{m}_i (\boldsymbol{\omega} \times \mathbf{r}_i)$$

is referred to by many authors as the jet damping term.

The xyz components of the moment equation (5) are

$$\begin{aligned} M_x + M_{Tx} &= I_{xy}(\omega_x \omega_z - \dot{\omega}_y) - I_{yz}(\omega_y^2 - \omega_z^2) - \\ &\quad I_{xz}(\dot{\omega}_z + \omega_x \omega_y) + I_x \dot{\omega}_x + (I_x - I_y)\omega_y \omega_z + \\ &\quad 2\omega_y \int (y v_y + z v_z) dm - 2\omega_y \int y v_x dm - \\ &\quad 2\omega_z \int z v_x dm + \int (y \dot{v}_z - z \dot{v}_y) dm + a_{0y} \int y dm - a_{0y} \int z dm \quad (9) \end{aligned}$$

$$\begin{aligned} M_y + M_{Ty} &= I_{yz}(\omega_x \omega_y - \dot{\omega}_z) - I_{xz}(\omega_z^2 - \omega_x^2) - \\ &\quad I_{xy}(\dot{\omega}_x + \omega_y \omega_z) + I_y \dot{\omega}_y + (I_x - I_z)\omega_x \omega_z + \\ &\quad 2\omega_y \int (z v_z + x v_x) dm - 2\omega_x \int z v_y dm - 2\omega_x \int x v_z dm + \\ &\quad \int (z \dot{v}_x - x \dot{v}_z) dm + a_{0x} \int z dm - a_{0x} \int x dm \quad (10) \end{aligned}$$

$$\begin{aligned} M_z + M_{Tz} &= I_{xz}(\omega_y \omega_z - \dot{\omega}_x) + I_{xy}(\omega_y^2 - \omega_x^2) - \\ &\quad I_{yz}(\dot{\omega}_y + \omega_x \omega_z) + I_z \dot{\omega}_z + (I_y - I_x)\omega_x \omega_y + \\ &\quad 2\omega_z \int (x v_x + y v_y) dm - 2\omega_x \int x v_z dm - 2\omega_y \int y v_z dm + \\ &\quad \int (x \dot{v}_y - y \dot{v}_x) dm + a_{0y} \int x dm - a_{0z} \int y dm \quad (11) \end{aligned}$$

where components of vectors are denoted by subscripts x, y, z , the I symbols are moments and products of inertia about 0, and the vector \mathbf{v} is the velocity of a mass particle relative to the xyz frame. In these equations, the terms with \mathbf{a}_0 are due to noncoincidence of the center of mass with the origin of the xyz axes ($\mathbf{a}_0 \equiv \ddot{\mathbf{R}}_0$).

B. Simplified Model of Gas Flow and Burning Process

Approaches to the jet damping problem differ in the approximate model used to represent the gas ejection process. Some treatments (Ref. 1 and 2, for example) assume that the centroid of the mass of burning propellant coincides with the centroid of the entire vehicle. This assumption, while appropriate for smaller rockets, is not applicable to the present problem because the payload satellite mass is concentrated very far forward. Reference 3 takes account of this effect, but treats only the case of constant mass flow

density along the rocket axis. The model used by Scott and Mitchell⁴ takes account of the displacement of the center of mass of the propellant from the vehicle center of gravity, and also of the fact that the mass flux is larger in the aft portion of the combustion chamber than in the forward portion. Reference 4 assumes that the center of mass of the over-all vehicle does not shift appreciably during burning. However, the formulation may be corrected readily.

The modified jet damping formula will now be derived along the lines of Ref. 4, but using a fixed coordinate system rather than the center of gravity system of the reference and including center of gravity motions. We use as an approximate model the geometry of Fig. 3 in which the x axis is the longitudinal spin axis of the rocket. We neglect the change in spin rate due to jet damping and consider only the damping of precessional motions about the y and z axes.

We assume uniform burning with relative velocity only along the x axis. The integral

$$\int x v_x dm$$

which appears in the moment equations can be rewritten as

$$\int x \{dm(x)/dt\} dx$$

so that, if $dm(x)/dt$ is a known function of x , it may be integrated. For uniform burning, the mass flow rate of the gas will increase with x so that a reasonable assumption is

$$\frac{dm(x)}{dt} = \dot{m} \left(\frac{x - l_m}{l_p} \right) \quad (12)$$

where \dot{m} is the terminal value at $x = l_m + l_p$. Thus

$$\int x v_x dm = \dot{m} \int_{l_m}^{l_m+l_p} x \left(\frac{x - l_m}{l_p} \right) dx = \dot{m} \left(\frac{l_p^2}{3} + \frac{l_p l_m}{2} \right) \quad (13)$$

With the origin of the xyz axes fixed in the missile, l_m is a constant. However, \bar{r} changes with time because of the mass burned. The change is easily computed to be

$$\bar{r}_x = \bar{x} = \frac{\dot{m} t [l_m + (l_p/2)]}{m} \quad (14)$$

$$\bar{r}_y = \bar{y} = 0$$

$$\bar{r}_z = \bar{z} = 0$$

where \bar{x} is negative for the axes chosen, and m is the instantaneous total mass. Note that effects of grain slotting are neglected.

Under thrust, the acceleration of the center of mass is

$$\mathbf{A}_{c.g.} = \ddot{\mathbf{R}}_0 + \dot{\omega} \times \bar{\mathbf{r}} + \omega \times (\omega \times \bar{\mathbf{r}}) + 2\dot{\omega} \times [\bar{\mathbf{r}}] + [\ddot{\mathbf{r}}] = -(T/m)\mathbf{i} \quad (15)$$

The center of mass remains on the x axis

$$\bar{\mathbf{r}} = \bar{x}\mathbf{i}$$

so that the foregoing equation for $\mathbf{A}_{c.g.}$ becomes

$$-(T/m)\mathbf{i} = \ddot{\mathbf{R}}_0 + [-\bar{x}(\omega_x^2 + \omega_y^2) + \ddot{x}]\mathbf{i} + [\bar{x}\dot{\omega}_z + \dot{x}\omega_x\omega_y + 2\dot{x}\dot{\omega}_z]\mathbf{j} + [\bar{x}\omega_x\omega_z - \dot{x}\dot{\omega}_y - 2\dot{x}\dot{\omega}_y]\mathbf{k}$$

Solving for $\ddot{\mathbf{R}}_0$

$$\ddot{\mathbf{R}}_0 = [-(T/m) + \bar{x}(\omega_x^2 + \omega_y^2) - \ddot{x}]\mathbf{i} - [\bar{x}(\dot{\omega}_z + \omega_x\omega_y) + 2\dot{x}\dot{\omega}_z]\mathbf{j} - [\bar{x}(\omega_x\omega_z - \dot{\omega}_y) - 2\dot{x}\dot{\omega}_y]\mathbf{k}$$

where $\ddot{\mathbf{R}}_0$ is the acceleration of the origin. The center of gravity shift term is then

$$-\ddot{\mathbf{R}}_0 \times \bar{\mathbf{r}} m = -\mathbf{a}_0 \times \bar{\mathbf{r}} m = m\bar{x} \{ [\bar{x}(\omega_x\omega_z - \dot{\omega}_y) - 2\dot{x}\dot{\omega}_y]\mathbf{j} - [\bar{x}(\dot{\omega}_z + \omega_x\omega_y) + 2\dot{x}\dot{\omega}_z]\mathbf{k} \} \quad (16)$$

Assuming a free symmetrical rocket with zero product of inertia, and substituting Eqs. (13-16) into the general component Eqs. (9-11), yields

$$M_x = I_x \dot{\omega}_x = 0 \quad (17)$$

$$M_y = I_y \dot{\omega}_y + (I_x - I) \omega_x \omega_z + 2\omega_y \dot{m} [(l_p^2/3) + (l_p l_m/2)] + m\bar{x} \{ \bar{x}(\omega_x \omega_z - \dot{\omega}_y) - 2\dot{x}\dot{\omega}_y \} \quad (18)$$

$$M_z = I_z \dot{\omega}_z + (I - I_x) \omega_x \omega_y + 2\omega_z \dot{m} [(l_p^2/3) + (l_p l_m/2)] - m\bar{x} \{ \bar{x}(\omega_x \omega_y + \dot{\omega}_z) + 2\dot{x}\dot{\omega}_z \} = 0 \quad (19)$$

where

$$I_y = I_z = I = I_{c.g.} + m\bar{x}^2$$

$$\bar{x} = \frac{\dot{m} t [l_m + (l_p/2)]}{m}$$

\dot{m} is the rate of change of total mass (a negative number). The first of these indicates that, for no jet damping in spin, $\omega_x = n = \text{const.}$ The second and third equations describe the pitching and yawing motions of the rocket. These equations differ from the more common forms as follows.

1) They do not contain derivatives of the moments of inertia, as do those of Refs. 1-3. Because the moments of inertia during burning are generally not known to good accuracy, it is important not to compound the error by the inaccurate process of differentiation. Use of Eq. (8) leads to forms involving derivatives of moments of inertia, a procedure that has been avoided.

2) They do not assume the center of gravity to be fixed in the body, as in Refs. 1-5.

C. Solutions of Equations of Motion

Equations (18) and (19) may be combined in complex form as follows:

$$M_y + iM_z = (I - m\bar{x}^2) \dot{\omega}_{yz} + [\dot{m}(\frac{2}{3}l_p^2 + l_p l_m) - 2m\bar{x}\dot{\bar{x}}] \omega_{yz} - i[(I_x - I)n + m\bar{x}^2 n] \omega_{yz} = 0 \quad (20)$$

where $\omega_{yz} = \omega_y + i\omega_z$, and $i = (-1)^{1/2}$.

Rearranging, and defining

$$P(t) = (\dot{m}/I_{c.g.})(\frac{2}{3}l_p^2 + l_p l_m) - (2m\bar{x}\dot{\bar{x}}/I_{c.g.}) \quad (21)$$

$$Q(t) = [(I_x/I_{c.g.}) - 1]n \quad (22)$$

$$\dot{\omega}_{yz} + [P(t) - iQ(t)] \omega_{yz} = 0 \quad (23)$$

The last equation is easily integrated as

$$\omega_{yz}(t) = \omega_{yz}(0) \exp \left[- \int_0^t P(t) dt \right] \exp \left[i \int_0^t Q(t) dt \right] \quad (24)$$

The frequency of oscillation is established by the term

$$\exp \left[i \int_0^t Q(t) dt \right]$$

and the amplitude damping is established by the term

$$\exp \left[- \int_0^t P(t) dt \right]$$

Because the quantity measured in flight is one component of the angular acceleration normal to the nominal spin axis ω_{yz} , the equations of motion will be solved for this quantity rather than for some other measure of the attitude. It is

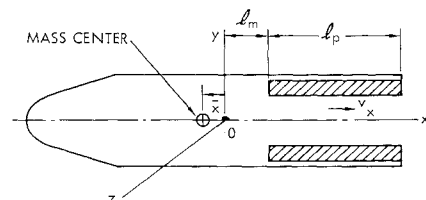


Fig. 3 Approximate model for burning process.

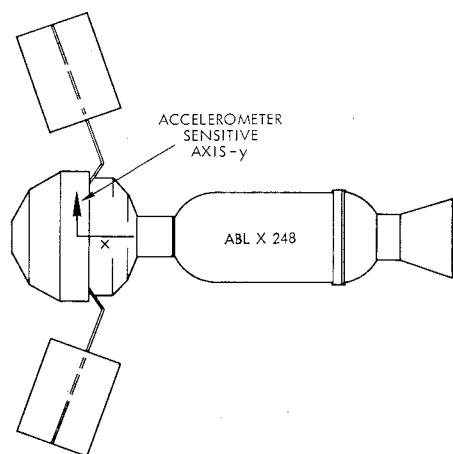


Fig. 4 Explorer VI third stage and satellite payload.

shown in the next section that the angular acceleration is readily related to the instantaneous attitude of the vehicle.

$\dot{\omega}_{yz}$ is found by substituting Eq. (23) into Eq. (24). We obtain

$$\dot{\omega}_{yz} = \dot{\omega}_{yz}(0) \left[\frac{P(t) - iQ(t)}{P(0) - iQ(0)} \right] \exp \left[-\int_0^t P(t) dt \right] \times \exp \left[i \int_0^t Q(t) dt \right] \quad (25)$$

and the envelope of the $\dot{\omega}_{yz}(t)$ vs t curve is found to be

$$\dot{\omega}_{yz}(0) \left[\frac{P(t)^2 + Q(t)^2}{P(0)^2 + Q(0)^2} \right]^{1/2} \exp \left[-\int_0^t P(t) dt \right] \quad (26)$$

IV. Experimental Data

The satellite Explorer VI, launched August 7, 1959, carried an angular accelerometer that measured one component of the vehicle angular acceleration normal to the nominal spin axis (see Fig. 4). The third stage of the Thor-Able launch vehicle was the spin-stabilized Allegany Ballistics Laboratory X-248A-4 solid rocket. The angular acceleration signal measured during the burning period of the third stage was an oscillating quasi-sinusoid with zero shift. The envelope of the oscillatory portion is plotted in Fig. 1. The fact that an oscillating component of angular acceleration was present indicates that the vehicle was executing a conical free precession or wobble in space (Fig. 5). Since aerodynamic forces were negligible (altitude about 800,000 ft), the gradual reduction in the precession amplitude could only have been caused by jet damping.

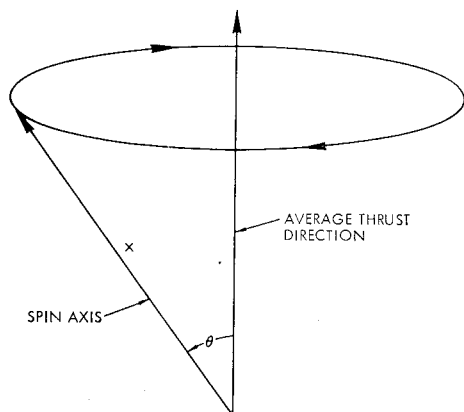


Fig. 5 Free precessional motion.

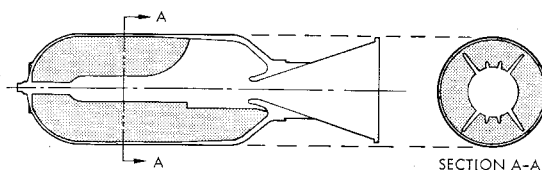


Fig. 6 X-248 internal geometry.

The approximate magnitude of the initial cone angle may be estimated from the angular acceleration record by assuming that the vehicle is symmetric and neglecting cone angle change due to jet damping over one precession cycle. The vehicle angular momentum is then conserved and it may be shown⁶ that the half cone angle θ defined in Fig. 5 is given by

$$\tan \theta = (I_{c.g.} |\omega_{yz}|) / I_x n \quad (27)$$

and that the component of angular velocity about the accelerometer axis is given by

$$\omega_y = |\omega_{yz}| \cos \left[\left(\frac{I_x - I_{c.g.}}{I_{c.g.}} \right) nt - \phi \right] \quad (28)$$

where ϕ is an arbitrary phase angle.

Differentiating Eq. (28), taking absolute values and substituting from Eq. (27), we obtain

$$\tan \theta = \frac{I_{c.g.}^2}{I_x (I_{c.g.} - I_x)} \frac{|\dot{\omega}_y|}{n^2} \quad (29)$$

indicating that the tangent of the cone angle is proportional to the amplitude of the oscillating angular acceleration component.

Substitution of the appropriate numerical values into Eq. (29) results in a value $\theta = 6.4^\circ$ for the cone angle at 2.9 sec of burning.

The initial cone angle was presumably produced by a lateral tipoff impulse applied at staging or at third-stage ignition. This tipoff may be partially due to the asymmetric thrust rise characteristics of the X-248. The value of tipoff impulse which would produce this cone angle, about 6 lb-sec at the nozzle, is somewhat larger than those observed in ground tests on the X-248.⁷ Other sources of tipoff are unknown. The frequency of the angular acceleration signal agreed well with the frequency predicted by Eq. (28) throughout the period of burning.

V. Comparison of Theory and Experiment

To compare the theory developed in Sec. III with the flight data, the functions $P(t)$ and $Q(t)$ were computed approximately for the X-248 and substituted into Eq. (26) for the envelope of the normal angular acceleration. The initial value of peak-to-peak angular acceleration was selected to agree with that observed at 2.9 sec of burning time. Staging occurred 0.015 sec after rocket ignition, but the first portion of the trace is uncertain because of accelerometer response to the staging transient. In evaluating P and Q , the complex grain geometry of the X-248 (Fig. 6) was simplified by neglecting the slots in the grain and computing moments of inertia on the basis of a hollow cylinder of varying inside diameter. The resulting approximate values for the inertias and center of gravity deviation are shown in Fig. 7. Weight flow rate was assumed constant at its average value, 12.4 lb/sec.

VI. Discussion

The comparison of the damping rates given by theory and flight test is given in Fig. 1. In general, agreement is quite good over most of the range of burning. The transient observed at the end of burning is not predicted by the theory.

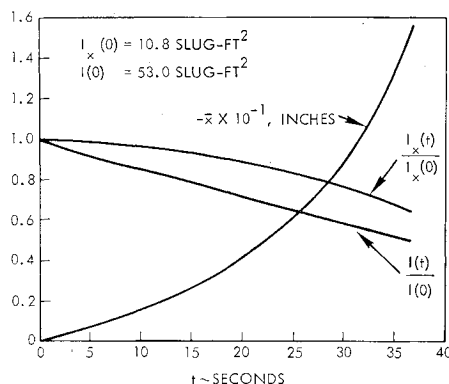


Fig. 7 Explorer VI third-stage vehicle—mass properties data.

This disagreement possibly may be due to the increased importance of thrust misalignment toward the end of burning.

The analysis, of course, contains a number of unavoidable assumptions. Among these are the following.

1) Approximate grain geometry is assumed. Fortunately, the damping formula, Eq. (26), is not unduly sensitive to small parameter variations. Alternate damping formulas arising from Eq. (8), which contain derivatives of the inertias, give unacceptable accuracy.

2) The vehicle was assumed to be rigid. The actual rocket vehicle contained two nonrigid components. An annular viscous damper of the type described in Ref. 8 was incorporated into the spacecraft to damp free precession after burning. Its effects during burning are considered negligible because of the much higher moments due to jet damping forces. (The effect of the annular damper would be to increase, rather than diminish, the cone angle.) Because of a malfunction, one of the four solar cell paddles of the satellite was not rigidly locked, but could move a few degrees about its hinge axis. Again, the effect would be to increase the cone angle.

3) Jet damping about the roll axis was neglected. The

spin rate as measured by signal strength fluctuations remained constant within about 4% at 2.84 rev/sec.

4) Thrust misalignment effects were neglected. The effect of thrust misalignment is to add additional terms to the right side of Eq. (25). One additional term is slowly varying and the other oscillates at the same angular frequency $Q(t)$, as do the free precession terms. The thrust misalignment terms have been evaluated numerically for an assumed nominal thrust misalignment and found to be negligible except for about the last 5 sec of burning. Since the actual misalignment is an unknown quantity the effect cannot be evaluated precisely.

Within the limitations described, the foregoing analysis provides a sufficiently accurate estimate of the wobble reduction due to jet damping. It is probable that the damping expression, Eq. (26), can be used to predict wobble reduction during burning for other spin-stabilized solid stages.

References

- ¹ Davis, L., Jr., Follin, J. W., Jr., and Blitzer, L., *Exterior Ballistics of Rockets* (D. Van Nostrand Co., Inc., New York, 1958), p. 33.
- ² Rosser, J. B., Newton, R. R., and Gross, G. L., *Mathematical Theory of Rocket Flight* (McGraw-Hill Book Co., Inc., New York, 1947), p. 134.
- ³ Barton, M. V., "The effect of variation of mass on the dynamic stability of jet propelled missiles," *J. Aeronaut. Sci.* **17**, 197-203 (1950).
- ⁴ Scott, P. B. and Mitchell, D. H., "A preliminary consideration of the powered flight dynamics of an unguided rolling missile," *Space Technology Labs. STL/TM-60-0000-19104* (1960).
- ⁵ Leon, H. I., "Spin dynamics of a thrusting rocket in vacuum," *Proceedings of the Fourth Midwestern Conference on Solid Mechanics* (University of Texas, Austin, Texas, 1959).
- ⁶ Thomson, W. T., *Introduction to Space Dynamics* (John Wiley and Sons, Inc., New York, 1963), p. 116.
- ⁷ Gungle, R. L., Brosier, W. S., and Leonard, H. W., "An experimental technique for the investigation of tipoff forces associated with stage separation of multistage rocket vehicles," *NASA TN D-1030* (March 1962).
- ⁸ Carrier, G. F. and Miles, J. W., "On the annular damper for a freely precessing gyroscope," *J. Appl. Mech.* **27**, 237-240 (1960).